

Supramolecular Hydrogels with Reverse Thermal Gelation Properties from (Oligo)tyrosine Containing Block Copolymers

Jin Huang,[†] Conn L. Hastings,[‡] Garry P. Duffy,[‡] Helena M. Kelly,[§] Jaclyn Raeburn,^{||} Dave J. Adams,^{||} and Andreas Heise^{*†}

[†]School of Chemical Sciences, Dublin City University, Dublin 9, Ireland

[‡]Department of Anatomy and [§]School of Pharmacy, The Royal College of Surgeons in Ireland, 123 St. Stephens Green, Dublin 2, Ireland

^{||}Department of Chemistry, University of Liverpool, Crown Street, Liverpool, L69 7ZD, United Kingdom

S Supporting Information

ABSTRACT: Novel block copolymers comprising poly(ethylene glycol) (PEG) and an oligo(tyrosine) block were synthesized in different compositions by *N*-carboxyanhydride (NCA) polymerization. It was shown that PEG2000-Tyr₆ undergoes thermoresponsive hydrogelation at a low concentration range of 0.25–3.0 wt % within a temperature range of 25–50 °C. Cryogenic transmission electron microscopy (Cryo-TEM) revealed a continuous network of fibers throughout the hydrogel sample, even at concentrations as low as 0.25 wt %. Circular dichroism (CD) results suggest that better packing of the β -sheet tyrosine block at increasing temperature induces the reverse thermogelation. A preliminary assessment of the potential of the hydrogel for in vitro application confirmed the hydrogel is not cytotoxic, is biodegradable, and produced a sustained release of a small-molecule drug.



INTRODUCTION

Hydrogels are critical materials in biomedical science. Their high water content and permeability, allied to structural integrity, similar to the extracellular matrix, means that hydrogels are ideal building blocks in regenerative medicine and as therapeutic delivery systems.¹ Despite the immense progress made in the development of hydrogels, their first clinical applications and the large and diverse number of materials disclosed in the academic and patent literature, there is still a high demand for the development of new hydrogels with material properties that better match application demands. Of particular interest are reverse thermoresponsive gels, that is, solutions, which transform into a gel upon temperature increase.² In particular, thermoresponsive hydrogels are highly amenable to the localized delivery of small-molecule drugs and other therapeutic molecules due to their tendency to maintain a liquid state at room temperature, thereby enabling a minimally invasive administration via syringing and subsequent ability to rapidly form a robust gel bolus upon heating to physiological temperature, thereby enforcing drug cohesion and facilitating sustained release at the intended site of action. Such systems can potentially achieve local efficacy for extended periods, requiring the administration of smaller doses, thereby reducing the manifestation of off-target effects associated with systemic administration of drugs.³

A promising class of materials is that of synthetic hydrogels obtained by self-assembly of amphiphilic polypeptides.⁴ Amphiphilic peptides can self-assemble into the supramolecular

hydrogel matrix through noncovalent interactions such as hydrogen bonding, electrostatic interactions, π -stacking, and hydrophobic interactions.⁵ A prominent example is the peptide amphiphiles introduced by Stupp consisting of a hydrophobic chain segment attached to a hydrophilic amino acid sequence.⁶ This design promotes supramolecular self-assembly into three-dimensional networks of fibrils in aqueous solution, stabilized through peptide interactions at a low concentration. While this design concept is very efficient, the self-assembly process is highly sensitive to the length and sequence of the amino acid block and relies on tedious multistep peptide and organic synthesis.⁷

Utilizing a polymerization approach would potentially simplify the synthetic efforts, however, at the expense of monodispersity and the oligopeptide sequence. Synthetic polypeptides can readily be prepared by the ring-opening polymerization of amino acid *N*-carboxyanhydrides (NCA).⁸ Recent advances demonstrate the feasibility of NCA polymerization for the synthesis of complex polymer structures capable of self-assembly,⁹ some of which are reported to form hydrogels. For example, Deming employed NCA polymerizations for the synthesis of hydrogel forming diblock copolypeptide amphiphiles.¹⁰ These materials contain water-soluble polyelectrolyte blocks such as poly(L-lysine) or poly(L-

Received: October 22, 2012

Revised: November 26, 2012

glutamate) and an α -helical poly(L-leucine) hydrophobic block. The gelation is driven by the stiff α -helical conformation of the hydrophobic domain and the electrostatic repulsion from the polyelectrolyte segments. However, hydrogelation was only achieved when both the hydrophobic and hydrophilic segments had a sufficiently high molecular weight. Jeong reported a series of amphiphilic hybrid block copolymers obtained by ring-opening polymerization of alanine or phenylalanine NCAs.¹¹ These materials self-assemble into nanostructures such as micelles in aqueous solutions and further transition into hydrogels at high polymer concentration in the range of 3.0–14 wt % through intermicellar aggregation when the temperature increases. Very recently, Chen also reported micelle-assembled thermosensitive hydrogels based on poly(L-glutamate)s bearing different hydrophobic side groups via NCA polymerization. Depending on the nature of the side chains, the polymers underwent sol–gel transitions with increasing temperature up to 62 °C at high polymer concentration (typically 9.0 wt %).¹²

We were interested to investigate if the advantages of NCA polymerization for the synthesis of amphiphilic polypeptides could be married with efficient hydrogelation at low concentration and thermoresponsive behavior. In this concept, a single amino acid must be able to display multiple modes of interaction, triggering self-assembly into the hydrogel matrix through noncovalent interactions. We hypothesized that tyrosine is a promising amino acid candidate. Despite its polar phenol group in the side chain, tyrosine residues are relatively hydrophobic when the pH of the solution is lower than the pK_a of the phenol.¹³ In addition to the ability to form stable β -sheet assemblies through a main chain amide bond driven hydrogen bonding, it has been shown that hydrogen bonding from the tyrosine –OH group contributed favorably to protein stability.¹⁴ Because one of the two lone electron pairs is partially delocalized within the aromatic ring, it can act either as hydrogen bonding donor or acceptor.¹⁵ Baker and Hubbard revealed that Tyr-OH groups form more hydrogen bonds to water molecules than intramolecular hydrogen bonds; although, in proteins, the tyrosine phenolic hydroxyl group generally forms a single intramolecular hydrogen bond with a main-chain carbonyl oxygen or a side chain carboxyl group.¹⁶ If desired, tyrosine can also be enzymatically cross-linked¹⁷ for hydrogel stabilization.¹⁸

To explore if the unique features of tyrosine can be utilized to trigger supramolecular hydrogel formation at low concentration, we designed a range of PEG conjugated tyrosine-based amphiphiles by simple NCA polymerization. The hydrogelation profile is highly sensitive to the polymer composition and the materials display rare reverse thermogelation. We determine the applicability of this polymer to form an injectable drug delivery vehicle and undertake a preliminary appraisal of the biodegradability and toxicity of the formulation in cultured cells. The release of a model compound, desferrioxamine (DFO), a small-molecule pro-angiogenic, from the thermoresponsive gel was investigated.

EXPERIMENTAL SECTION

Materials. All chemicals were purchased from Sigma-Aldrich and used as received unless otherwise noted. *O*-Benzyl-L-tyrosine and phenylalanine were supplied by Bachem. Anhydrous DMF, ethyl acetate, and THF were used directly from the bottle under an inert and dry atmosphere.

O-Benzyl-L-tyrosine (Tyr-NCA) and Phenylalanine (Phe-NCA). α -Pinene (15 g, 110.3 mmol) and *O*-benzyl-L-tyrosine (10.0 g, 36.9 mmol) were dissolved in 80 mL of anhydrous ethyl acetate in a three-neck round-bottomed flask. The mixture was stirred and heated to reflux with a slow flow of nitrogen. Then, a solution of triphosgene (5.5 g, 18.4 mmol) in anhydrous ethyl acetate (40 mL) was added dropwise. Two-thirds of the solution was added within 1 h after which the reaction was left at reflux for another hour. The rest of the triphosgene solution was added until the reaction mixture became clear. Subsequently, around 60 mL of the solvent was removed under pressure and 120 mL of *n*-heptane was added slowly to precipitate NCA. After filtration, the solid was recrystallized from ethyl acetate and *n*-heptane (1:2) four times until the NCA was recovered as an off-white crystal. Yield: 8.2 g (75%). ¹H NMR (400 MHz, CDCl₃, δ , ppm): 2.95 (dd, J = 14.13, 8.36 Hz, 1H, -CH-CH₂-), 3.21 (dd, J = 14.13, 4.10 Hz, 1H, -CH-CH₂-), 4.49 (dd, J = 4.10, 8.36 Hz, 1H, -NH-CH-), 5.04 (s, 2H, -CH₂-O-), 5.96 (s, 1H, -NH-CH-), 6.95 (d, J = 8.61 Hz, 2H, ArH), 7.10 (d, J = 8.61 Hz, 2H, ArH), 7.39 (m, 5H, ArH). ¹³C NMR (400 MHz, CDCl₃, δ , ppm): 37.1 (-CH-CH₂-), 58.9 (-CH-CH₂-), 70.0 (-O-CH₂-), 115.6 (Ar), 125.9 (Ar), 127.5 (Ar), 128.1 (Ar), 128.7 (Ar), 130.2 (Ar), 136.6 (Ar), 151.5 (Ar), 158.5 (-O-C(O)-CH-), 168.6 (-C(O)-NH-).

The same procedure was applied to the synthesis of phenylalanine NCA. Yield: 5.3 g (45%). ¹H NMR (400 MHz, CDCl₃, δ , ppm): 2.99 (dd, J = 14.16, 8.59 Hz, 1H, -CH-CH₂-), 3.30 (dd, J = 14.16, 4.06 Hz, 1H, -CH-CH₂-), 4.54 (dd, J = 4.06, 8.59 Hz, 1H, -NH-CH-), 6.03 (s, 1H, -NH-CH-), 7.20 (m, 2H, ArH), 7.35 (m, 5H, ArH). ¹³C NMR (400 MHz, CDCl₃, δ , ppm): 38.0 (-CH-CH₂-), 58.9 (-CH-CH₂-), 128.2 (Ar), 129.3 (Ar), 129.4 (Ar), 134.0 (Ar), 151.8 (-O-C(O)-CH-), 168.7 (-C(O)-NH-).

General Procedure for the Synthesis of PEG-*b*-poly(*O*-benzyl-L-tyrosine). *O*-Benzyl-L-tyrosine NCA (715 mg, 2.4 mmol) was dissolved in 30 mL of dry DMF in a Schlenk tube. A solution of α -methoxy- ω -amino poly(ethylene glycol) (M_w = 2000 g/mol, PDI 1.03, 960 mg, 0.48 mmol) in 10 mL of dry DMF was added after the NCA had dissolved. The reaction was left to stir at room temperature for 4 days in a dry nitrogen atmosphere until NCA was completely consumed (as monitored by FTIR). The reaction mixture was precipitated into an excess diethylether, filtered, and dried under vacuum as a pale yellow solid (yield 80%). ¹H NMR of PEG2000-*b*-poly(*O*-benzyl-L-tyrosine)₆ (400 MHz, TFA-*d*⁶ with CDCl₃, δ , ppm): 2.66–3.03 (br m, 12H), 3.25–4.07 (br m, 176H), 4.5–5.17 (br m, 18H), 6.70–7.44 (br m, 54H).

PEG-*b*-poly(L-tyrosine). PEG-*b*-poly(*O*-benzyl-L-tyrosine) (1 g) was dissolved in 10.0 mL of hexafluoroisopropanol (HFIP) with 2 mL of trifluoroacetic acid (TFA). A 6-fold excess with respect to *O*-benzyl-L-tyrosine of 33% of HBr in acetic acid (1.6 mL) was added. After 16 h, the mixture was added dropwise into diethyl ether. The polymer was filtered and redissolved in deionized water and dialyzed against water for 7 days. The solution was lyophilized as a white fluffy powder (yield 55%). ¹H NMR of PEG2000-*b*-poly(L-tyrosine)₆ (400 MHz, TFA-*d*⁶, δ , ppm): 2.62–3.26 (br s, 12H), 3.30–4.23 (br m, 176H), 4.58–4.97 (br s, 6H), 6.70–7.27 (br m, 31H).

Hydrogel Preparation and Sol–Gel Transition. Hydrogel solutions were prepared by dissolving freeze-dried polypeptide samples in deionized water at the desired concentrations. The homogeneous solutions were obtained by sonication at 20 °C until the solutions became clear. The formation of the gel was determined via vial inverting method.¹⁹ Each sample at a given concentration was dissolved into distilled water in 2 mL vials. After equilibration at room temperature overnight, the vials containing samples were immersed in a water bath equilibrated at each given temperature for 15 min. The sol–gel transition was determined after inverting the vial. If no flow was observed within 1 min, the sample was regarded as a gel. For the temperature-dependent measurements, the temperature was raised in 1 °C steps (the precision of the sol–gel transition temperature was ± 1 °C). Each temperature data point represents an average of three measurements. The gelation time as a function of block copolymer concentration at the physiologically relevant temperature of 37 °C was measured in a 37 °C water bath. The

gelpoint was determined via vial inverting method every 15 min in the initial 3 h. Thereafter, the gelation was checked every 30 min. The duration from the time point the polymer solution was put into the water bath to the time point the gelation was observed was defined as the gelation time. Each gelation time data point was determined from an average of three measurements.

Hydrogel Degradation Profile. Degradation of the hydrogel was assessed by measuring the weight loss every 24 h for nine days in triplicate. A 1 mL aliquot of deionized water containing 1.0 and 2.0 wt % block copolymer, respectively, was placed in a vial and left in a water bath at 37 °C for 30 min to allow gelation to occur. A 2 mL aliquot of prewarmed Krebs buffer solution was gently added into each vial, taking care not to disturb the hydrogels. The vials were then left in the water bath for the duration of the degradation study. Every 24 h, the Krebs buffer solution was removed along with any gel debris that had accumulated. Vials were then weighed to assess the change in weight of the hydrogels over the duration of the study. In the enzymatic degradation experiment, the enzymes were doped into the hydrogel by dissolving the enzymes in the 5 mg/mL (~0.5 wt %) polymer solution. The activity of both enzymes in the final polymer solution is 28.5 unit/mL. The hydrogelation was triggered by heating the solutions to 37 °C in a water bath (around 4 h). The formation of the hydrogel was determined by the vial inverting method.

Desferrioxamine (DFO) Release Experiment. Analysis of DFO release from a 2.0 wt % (20 mg/mL) PEG2000-Tyr₆ hydrogel was undertaken as previously described.²⁰ Hydrogels containing DFO of 100 μM concentrations were prepared. A total of 2 g of 20 mg/mL polymer with 100 μM DFO was placed in each of three glass vials and allowed to gel in a water bath for 2 h at 37 °C. A 1 mL aliquot of phosphate buffer (pH 7.2) was added to each vial and the samples were allowed to incubate at 37 °C while shaking at 75 rpm for the duration of the release study (2 mL of buffer was used at 4 and 24 h to ensure appropriate sink conditions in release media at early time points). The phosphate buffer was completely removed and replaced at 4 h, 24 h, day 3, day 5, and day 7 and frozen until analysis. All studies were performed in triplicate. Samples were analyzed for DFO content via HPLC.

Hydrogel Biocompatibility. The biocompatibility of the hydrogel was preliminarily assessed through the culture of cell monolayers on a preformed PEG2000-Tyr₆ hydrogel substrate. Mesenchymal stem cells were derived from bone marrow aspirates of Wistar rats (rMSCs) under ethical approval. Cells were cultured in Dulbecco's modified Eagles medium (DMEM) supplemented with 10% fetal bovine serum (FBS), 1% L-glutamine, 2% penicillin/streptomycin, 1% nonessential amino acids, and 0.5% Glutamax. A total of 50000 rMSCs were seeded on a preformed gel layer consisting of 100 μL of 2.0 wt % gel allowed to set at 37 °C for 1 h in wells of a 24-well plate. Cell viability and morphology was assessed qualitatively at 48 h, as previously described,²¹ through use of a Live/Dead stain (Molecular Probes), which labels cells with calcein or ethidium homodimer to stain live cells green and dead cells red. The proportion of live to dead cells and the ability of cells to spread and attach to the gel substrate was assessed qualitatively through visual inspection of stained cells at 48 h.

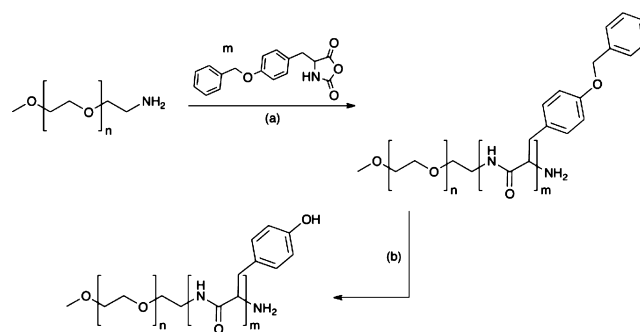
Methods. ATR-FTIR spectra were collected on a Perkin-Elmer Spectrum 100 in the spectral region of 650–4000 cm⁻¹ and were obtained from 16 scans with a resolution of 2 cm⁻¹. A background measurement was taken before the sample was loaded onto the ATR unit for measurements. CD data were collected on a Jasco J-810 CD spectrometer (Japan Spectroscopic Corporation) with a path length of 0.1 cm and a bandwidth of 1 nm. Three scans were conducted and averaged between 185 and 350 nm at a scanning rate of 20 nm min⁻¹ with a resolution of 0.2 nm. The data were processed by subtracting solvent as background. CD temperature-dependent measurements were performed on a Jasco J-815 spectropolarimeter (Japan Spectroscopic Corporation) with a PFD-425S/15 Peltier-type temperature controller with a temperature range from 10 to 60 °C and a temperature slope of 1 °C/min. The solution was allowed to equilibrate for 10 min at each temperature prior to data collection. The measurements were done between 185 and 350 nm in a 0.1 mm quartz cell. Dynamic rheological experiments were measured using an

Anton Paar Physica MCR101 rheometer. For the oscillatory shear measurements, a sandblasted parallel top plate with a 25 mm diameter and 1.0 mm gap distance were used. Evaporation of water from the hydrogel was minimized by covering the sides of the plate with low viscosity mineral oil. The measurements of storage modulus (G') and loss modulus (G'') with gelation were made as a function of time at a frequency of 1.59 Hz (10 rad/s) and at a constant strain of 2% as the temperature increased from 25 to 60 °C by a heating rate of 1.0 °C/min. A frequency sweep (1–100 Hz) was performed on the recovered gel at a constant strain of 2%. The morphology images of hydrogel were obtained by using a Hitachi S3400n SEM instrument. The preparation of samples for SEM analysis involved placing a drop of hydrogel on the thin carbon-coated film. The hydrogel was subjected to shock-freezing by liquid nitrogen, followed by lyophilization for 2 h. It was then submitted to a SEM scan after gold-coating for 2 min. Cryogenic–transmission electron microscopy (Cryo-TEM): Sample preparation was carried out using a CryoPlunge 3 unit (Gatan Instruments) employing a double blot technique. A total of 3 μL of sample was pipetted onto a plasma etched (15 s) 400 mesh holey carbon grid (Agar Scientific) held in the plunge chamber at approximately 90% humidity. The samples were blotted from both sides for 0.5, 0.8, or 1.0 s, dependent on sample viscosity. The samples were then plunged into liquid ethane at a temperature of –170 °C. The grids were blotted to remove excess ethane then transferred under liquid nitrogen to the cryo TEM specimen holder (Gatan 626 cryo holder) at –170 °C. Samples were examined using a Jeol 2100 TEM operated at 200 kV and imaged using a GatanUltrascan 4000 camera; images captured using Digital Micrograph software (Gatan). High-performance liquid chromatography (HPLC) for DFO release studies was performed on an Agilent 1120 Compact LC with a Phenomenex Gemini 5u C18 column, mobile phase acetonitrile/phosphate buffer (10/90% v/v), containing 2 mol ethylenediaminetetraacetic acid (EDTA), pH adjusted to 6.5 and UV detection at 440 nm. ¹H and ¹³C NMR spectra were recorded at room temperature with a Bruker Avance 400 (400 MHz). CF₃COOD and CDCl₃ were used as solvents and signals were referred to the signal of residual protonated solvent signals.

RESULTS AND DISCUSSION

Poly(ethylene glycol-*b*-O-benzyl-L-tyrosine) (PEG-PBTyr) block copolymers were synthesized by ring-opening polymerization of O-benzyl-L-tyrosine NCA using α -methoxy- ω -amino poly(ethylene glycol) ($M_w = 2000$ and 5000 g/mol) as the macroinitiator (Scheme 1). The ratio of PEG macroinitiator to NCA was systematically varied to obtain block copolymers with different block lengths ratios (Table 1). ¹H NMR analysis confirmed the very good agreement between the PEG to NCA monomer feed ratio with the composition of the obtained block copolymers, although, for PEG5000, a slight deviation was

Scheme 1. Synthesis of PEG/Tyr Block Copolymers^a



^aReagents and conditions: (a) DMF, 0 °C; (b) HBr/acetic acid, hexafluoroisopropanol/TFA, r.t.

Table 1. Characteristics of Poly(ethylene glycol-*b*-L-tyrosine) (PEG-Tyr) Obtained by Macroinitiation of *O*-Benzyl-L-tyrosine NCA from Amine-Functionalized PEG (PEG-NH₂)

PEG-NH ₂	feed ratio PEG/NCA ^a	composition block copolymer ^b
PEG2000	1:5	PEG2000-Tyr ₆
PEG2000	1:10	PEG2000-Tyr ₁₀
PEG2000	1:15	PEG2000-Tyr ₁₄
PEG5000	1:10	PEG5000-Tyr ₉
PEG5000	1:15	PEG5000-Tyr ₁₃
PEG5000	1:20	PEG5000-Tyr ₁₆
PEG5000	1:30	PEG5000-Tyr ₂₃

^aMolar ratio of PEG macroinitiator to *O*-benzyl-L-tyrosine NCA.

^bCalculated from ¹H NMR (CF₃COOD) using the integrated peak area ratios of the PEG ethylene signals at 3.30–4.23 ppm and the C_α signal of poly(L-tyrosine) at 4.58–4.97 ppm while using the aromatic groups at 6.70–7.27 ppm and C_β signal at 2.62–3.26 ppm of poly(L-tyrosine) as the internal standards.

observed at higher ratios. The subsequent quantitative deprotection of the tyrosine benzyl ether was monitored by ¹H NMR spectroscopy by the disappearance of the benzyl ether peaks (7.2–7.4 ppm) and afforded the poly(ethylene glycol-*b*-L-tyrosine) (PEG-Tyr).

After deprotection of the PEG5000 series, PEG5000-Tyr₂₃ was water insoluble, while all other block copolymers were readily soluble but did not form hydrogels at room temperature, even at polymer concentrations >120 mg/mL (12 wt %, higher concentrations were not investigated). Of the PEG2000 series, both PEG2000-Tyr₁₀ and PEG2000-Tyr₁₄ were water insoluble. PEG2000-Tyr₆, on the other hand, formed transparent hydrogels in deionized (DI) water at a range of concentrations and temperatures. Cryogenic transition electron microscopy (cryo-TEM) revealed a continuous network of fibers throughout the hydrogel sample, even at concentrations as low as 0.25 wt % (Figure 1). The fibers appear

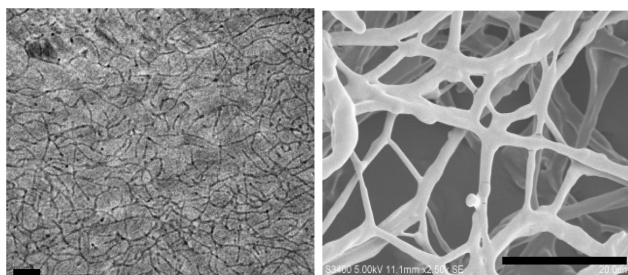


Figure 1. (Left) Cryogenic transmission electron microscopy (Cryo-TEM) images of PEG2000-Tyr₆ hydrogels at concentrations of 0.25 wt %; the scale bar represents 200 nm. (Right) Scanning electron microscopy (SEM) images of PEG2000-Tyr₆ hydrogel (0.5 wt %) after lyophilization; the scale bar represents 20 μm.

interconnected by cross-link points. SEM images of samples treated with liquid nitrogen followed by lyophilization to preserve the hydrogel structure also confirm the three-dimensional interconnected network structure (Figure 1).

Interestingly, the sol–gel phase diagram revealed a temperature-dependent profile at low solid content. Figure 2 shows that PEG2000-Tyr₆ undergoes thermoresponsive gelation at a concentration range of 0.25–3.0 wt % within a temperature range of 25 to 50 °C. The sol-to-gel transition temperature depends on the polymer concentration and increases with decreasing polymer concentration, for example, 28 °C at 2.0 wt

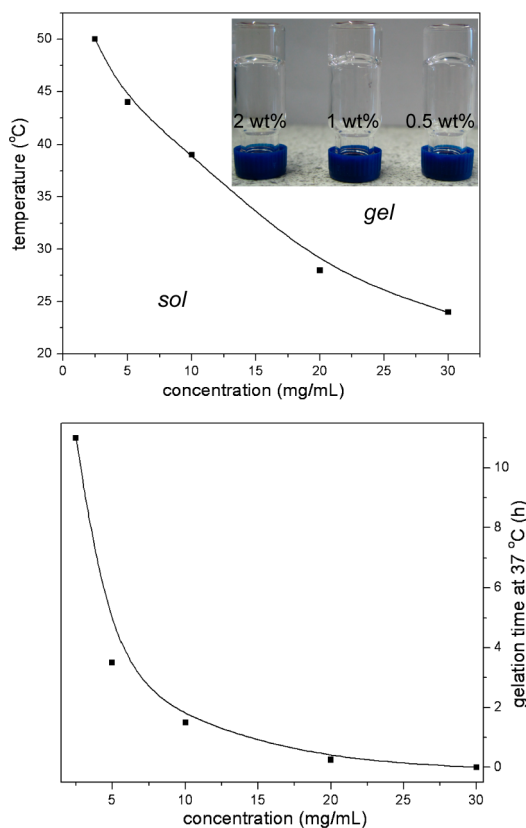


Figure 2. Hydrogelation temperature as a function of PEG2000-Tyr₆ concentration (top). Hydrogelation time as a function of PEG2000-Tyr₆ concentration at 37 °C (bottom).

% and 39 °C at 1.0 wt %. It is remarkable that even at a polymer concentration of 0.25 wt % stable hydrogels can be observed upon heating to 50 °C. The second phase diagram in Figure 2 depicts the gelation time as a function of block copolymer concentration at the physiologically relevant temperature of 37 °C. The data signify that the hydrogelation time can be completely controlled by the polymer concentration in water. Moreover, at concentrations >2.0 wt %, hydrogelation occurs immediately at this temperature. The thermogelation profile observed for PEG2000-Tyr₆ is contrary to most polypeptide aqueous systems that form a stable hydrogel via hydrogen bonding or ionic interactions at a low temperature and then undergo gel-to-sol transition (gel melting) when the temperature increases.^{22,23} Most relevant in that respect is the example of telechelic Fmoc-protected dityrosine end-capped PEG recently published by Hamley. Self-assembled β-sheet fibril-based hydrogels from these materials exhibited a gel-to-sol transition with increasing temperature.²⁴

All these results suggest that there is a very delicate block length ratio that needs to be met in this system for efficient hydrogel formation to occur because the hydrogelation was not observed for PEG2000-Tyr₁₀ and PEG2000-Tyr₁₄. An obvious explanation is the hydrophilic–hydrophobic balance between the PEG and the tyrosine block that is determining for the hydrogel formation.^{14,25} Moreover, the self-assembly of the PEG2000-Tyr₆ in water can to a large extent be ascribed to the β-sheet interaction in agreement with previously reported peptide hydrogels.²⁶ FTIR and CD spectra confirm that the tyrosine block adopts a typical β-sheet conformation when the hydrogel is formed as evident from the amide I band at 1623

cm^{-1} and the minimum at 220 nm in the CD spectrum. The hydrogels are stable up to pH 13, which coincides with the complete deprotonation of the tyrosine hydroxy groups (Supporting Information). Further evidence for the importance of the tyrosine phenolic groups in the current hydrogels was obtained from block copolymers in which the tyrosine was replaced by phenylalanine (Phe). Although the FTIR spectra of both PEG2000-Phe₅ and PEG2000-Phe₁₀ confirmed a β -sheet conformation, with a higher hydrophobicity index of 2.8 than Tyr (-1.3),²⁷ neither of the polymers were water-soluble and could form hydrogels. Apparently, the phenolic hydroxy groups render the tyrosine block more polar and better soluble than the phenylalanine block. This slight difference in structure favorably tips the amphiphilic balance and affects the self-assembly in aqueous solution. Furthermore, the partly polar phenolic group could promote intramolecular hydrogen bonds with water molecules or main-chain carbonyls and, thus, contributes to the molecular interaction in the hydrogels.¹⁶

While these results explain the hydrogel formation, they do not rationalize the reverse thermoresponsive sol-to-gel transition of PEG2000-Tyr₆. To investigate the conformational changes of the block copolymer in aqueous solution, temperature-dependent CD spectra were recorded. As revealed in Figure 3, the negative band at 220 nm, corresponding to β -

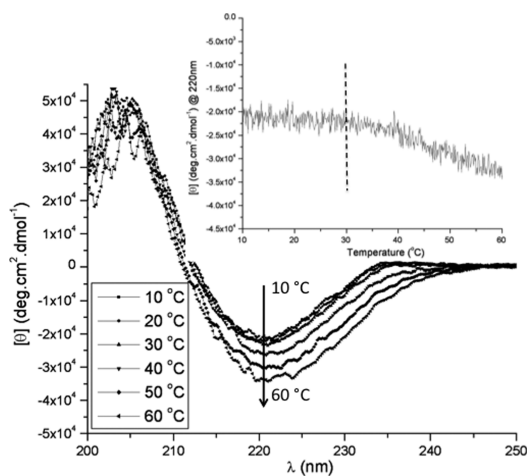


Figure 3. Circular dichroism spectra of PEG2000-Tyr₆ aqueous solution (0.25 mg/mL) as a function of temperature. Inset: Ellipticity change of PEG2000-Tyr₆ (0.25 mg/mL) at 220 nm as a function of temperature.

sheet conformation, gradually increased as the temperature increased from 10 to 60 °C, in particular, above 30 °C. This implies that the increment of β -sheet conformation at increased temperature increases, thereby promoting better intermolecular interaction and hydrogelation. We hypothesize that two phenomena contribute to this behavior. The first is the known dehydration of PEG at higher temperatures, causing the PEG blocks to become more hydrophobic.²⁸ This offsets the hydrophobic/hydrophilic balance in the block copolymer and decreases the molecular motion of the PEG block. On the other hand, an increase in temperature increases the molecular motion of the Tyr domain, promoting better phase packing and also enhancing its molecular self-organization via hydrogen bonding, as demonstrated by the stronger β -sheet conformation at elevated temperatures. This process facilitates block copolymer self-assembly and hydrogel network formation.

The sensitivity of the hydrogelation to the block lengths composition highlights the delicate balance of these interactions.

The viscoelastic properties of the gels were explored using oscillatory rheology, in which the temporal evolution of storage modulus (G') and loss modulus (G'') is typically measured to observe the gelation behavior.²⁹ Figure 4 shows the dynamic

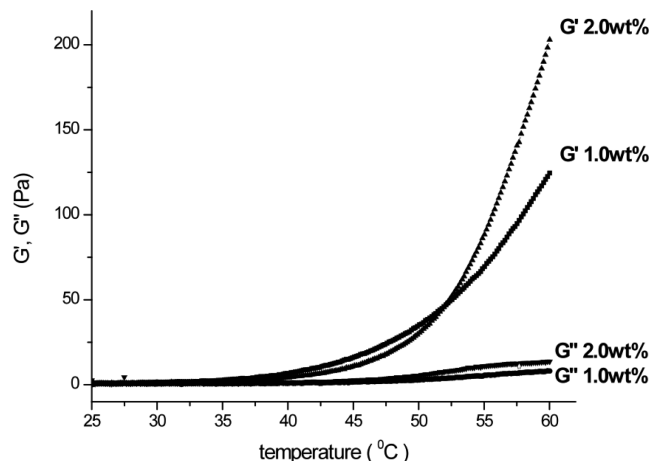


Figure 4. Dynamic mechanical changes in the modulus of PEG2000-Tyr₆ at 2.0 and 1.0 wt % as a function of temperature.

mechanical changes in the modulus of PEG2000-Tyr₆ at different concentration of 2.0 and 1.0 wt % as a function of temperature. The G' of the polymer in both cases is an order of magnitude higher than G'' as the temperature gradually increases from 25 to 60 °C. This is indicative of the formation of an elastic solid-like material as the temperature increases. At higher polymer concentrations, higher values of G' and G'' were obtained, indicating a more rigid gel. G' was found to be insensitive to the frequency in a range of 1–100 rad/s and only increase slightly with increasing frequency in all different concentrations (Supporting Information).³⁰

The information obtained from the spectroscopic and rheological analysis suggests that the hydrogel formation of PEG2000-Tyr₆ is collectively driven by several factors, including amphiphilic balance between PEG and Tyr blocks, hydrogen bonding by β -sheet conformation and phenolic group, and possibly also aromatic interaction from the side chains of poly(L-tyrosine). Better packing of the β -sheet tyrosine block at increasing temperature induces a reverse thermogelation. This is a desirable property for biomedical hydrogels because, at room temperature, a liquid gel-precursor solution could be administered by injection, possibly together with drugs or growth factors, followed by in situ gelling at body temperature, thus, avoiding surgical implantation.³ The applicability of PEG2000-Tyr₆ as biomedical hydrogels was therefore assessed in preliminary experiments.

Biostability and resorbability under simulated physiological condition are essential criteria in the assessment of biomedical hydrogels. The stability of the hydrogel at block copolymer concentrations of 2.0 and 1.0 wt % was measured in Krebs buffer solution. Krebs buffer is a physiological buffer that, to some degree, mimics the ionic composition, pH, and osmotic behavior of tissue fluid and, so, is a useful medium to examine the behavior of biomaterials in vitro. Figure 5 reveals a weight loss of around 20% and 5% after nine days for the gel of 1.0 and 2.0 wt %, respectively. While both hydrogels remained quite

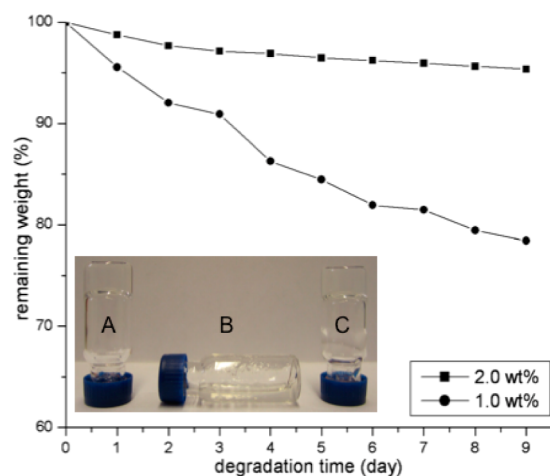


Figure 5. Weight loss of PEG2000-Tyr₆ hydrogel at 2.0 and 1.0 wt % in Krebs buffer solution. Inset: Degradation of hydrogels in the presence of (A) no enzyme, (B) chymotrypsin, and (C) trypsin. Enzymes (28.5 unit/mL) were incorporated in the hydrogel at 0.5 wt % in a 37 °C water bath; pictures taken after 7 days.

stable over the monitored time, the 2.0 wt % hydrogel displayed higher stability and lower weight loss due to its higher mechanical stability, as shown in Figure 4. This lack of mechanical strength of the 1.0 wt % hydrogel could allow for more uptake of water, resulting in more swelling, with concomitant structural breakdown. Second, a weaker gel will be more prone to mechanical disruption due to physical manipulation associated with buffer changes. Both of these factors together could account for the observed change in weight. In a second set of experiments, enzymes were encapsulated into the hydrogel (0.5 wt % block copolymer). Chymotrypsin was chosen as a positive control because it preferentially cleaves peptide amide bonds adjacent to an aromatic amino acid such as tyrosine, tryptophan and phenylalanine.³¹ Trypsin was selected as negative control as it cleaves peptide chains mainly at the carboxyl side of the amino acids lysine or arginine.³² The enzymes of 28.5 unit/mL were doped into the hydrogels by dissolving them in a 0.5 wt % polymer solution and subsequently triggering hydrogelation by heating to 37 °C. The hydrogel containing chymotrypsin showed a gradual disintegration within 24 h and completely broke into pieces after 7 days (inset of Figure 5). In contrast, no visible change was observed for the hydrogels containing trypsin or no enzyme in the same time period highlighting the selective enzymatic degradation by chymotrypsin. This experiment further shows that biomolecules can be incorporated without compromising the hydrogel formation.

We also explored the use of the hydrogel for the entrapment and release of small drug molecules. A 2.0 wt % PEG2000-Tyr₆ hydrogel was utilized to release the pharmacological pro-angiogenic desferrioxamine (DFO) over a period of 7 days.²⁰ DFO was dissolved within the gel as it is a water-soluble drug. Release of DFO from the hydrogel into phosphate buffer by diffusion at 37 °C was measured via HPLC. As shown in Figure 6, the gel produced a burst release within the first 24 h and then a sustained, albeit decreasing, release over the period of seven days. Interestingly, the gel released ~20% of the total encapsulated drug within seven days. However, the amount of drug released is sufficient to exert a biological effect.²⁰ The remainder of the drug may have become degraded, within both the gel and release buffer. The sustained release of the small-

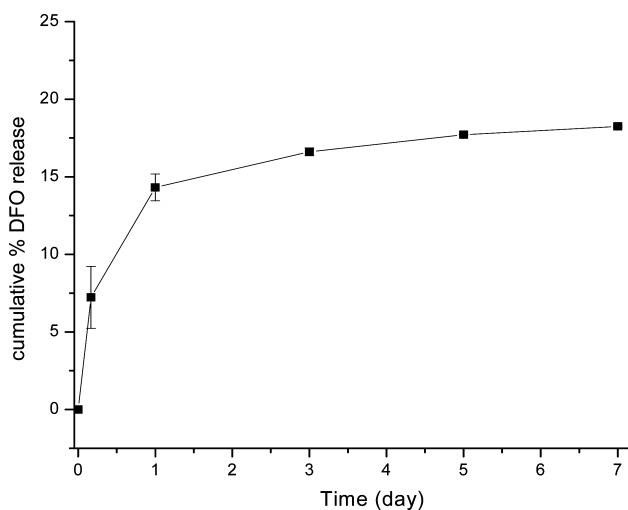


Figure 6. Cumulative release profile of DFO from 2.0 wt % hydrogel containing 100 μM DFO at 37 °C over seven days ($n = 3$, mean + standard deviation plotted).

molecule drug confirmed that the PEG2000-Tyr₆ hydrogel could potentially function as an injectable drug depot, which could exert sustained drug release and local efficacy for an extended period.

Finally, the cytotoxicity of the hydrogel was assessed by seeding rMSCs onto a preformed 2.0 wt % PEG2000-Tyr₆ gel layer and staining with a Live/Dead stain. No dead cells were apparent and cells were adherent to the gel layer, suggesting that the gel did not exert significant cytotoxicity after 48 h. At 48 h, the majority of cells appeared rounded, suggesting that the cells were not presented with sufficient attachment sites to enable spreading (Supporting Information).

CONCLUSIONS

Novel block copolymers comprising a PEG and an oligo-(tyrosine) block were synthesized in different compositions by NCA polymerization. The ability to form hydrogels is delicately dependent on the block length ratio with an optimum composition of PEG2000-Tyr₆. This material undergoes thermoresponsive gelation at a low concentration range of 0.25–3.0 wt % within a temperature range of 25 to 50 °C. The hydrogel formation of PEG2000-Tyr₆ is collectively driven by several factors including amphiphilic balance between PEG and Tyr blocks, hydrogen bonding by β -sheet conformation and phenolic group. CD analysis confirms that better packing of the β -sheet tyrosine blocks at increasing temperature induces the reverse thermogelation. A preliminary assessment of biocompatibility in vitro indicated that the hydrogel is not cytotoxic, is biodegradable, and produced a sustained release of a small-molecule drug. Therefore, this formulation may have potential as an injectable drug delivery vehicle.

ASSOCIATED CONTENT

Supporting Information

FTIR and CD spectra as a function of pH, frequency sweep, and storage modulus data for PEG2000-Tyr₆ hydrogels; cell toxicity image. This material is available free of charge via the Internet at <http://pubs.acs.org>.

AUTHOR INFORMATION

Notes

The authors declare no competing financial interest.

ACKNOWLEDGMENTS

Financial support from the Science Foundation Ireland (SFI) Principle Investigator Award 07/IN1/B1792 (J.H. and A.H.) is gratefully acknowledged. A.H. is a SFI Stokes Senior Lecturer (07/SK/B1241). The author would like to thank Anja Palmans from Eindhoven University of Technology and Anne Shanahan from Dublin Institute of Technology for the help with CD measurements. We thank Steve Fuzeland and Derek Atkins (Unilever R&D, Colworth, U.K.) for collecting the cryo-TEM data.

REFERENCES

- (1) (a) Vermonden, T.; Censi, R.; Hennink, W. E. *Chem. Rev.* **2012**, *112*, 2853. (b) Peppas, N. A.; Hilt, J. Z.; Khademhosseini, A.; Langer, R. *Adv. Mater.* **2006**, *18*, 1345. (c) Altunbas, A.; Pochan, D. J. *Top. Curr. Chem.* **2012**, *310*, 135. (d) Seliktar, D. *Science* **2012**, *336*, 1124. (e) Li, Y.; Rodrigues, J.; Tomás, H. *Chem. Soc. Rev.* **2012**, *41*, 2193.
- (2) (a) Li, Z. Q.; Guan, J. J. *Expert Opin. Drug Delivery* **2011**, *8*, 991. (b) Klouda, L.; Mikos, A. G. *Eur. J. Pharm. Biopharm.* **2008**, *68*, 34. (c) Jeong, B.; Kim, S. W.; Bae, Y. H. *Adv. Drug Delivery Rev.* **2002**, *54*, 37.
- (3) (a) Park, M. H.; Joo, M. K.; Choi, B. G.; Jeong, B. *Acc. Chem. Res.* **2012**, *45*, 42. (b) Moon, H. J.; Ko, D. Y.; Park, M. H.; Joo, M. K.; Jeong, B. *Chem. Soc. Rev.* **2012**, *41*, 4860. (c) Li, Z. Q.; Guan, J. J. *Expert Opin. Drug Delivery* **2011**, *8*, 991.
- (4) (a) Matson, J. B.; Stupp, S. I. *Chem. Commun.* **2012**, *48*, 26. (b) Branco, M. C.; Schneider, J. P. *Acta Biomater.* **2009**, *5*, 817.
- (5) (a) Estroff, L. A.; Hamilton, A. D. *Chem. Rev.* **2004**, *104*, 1201. (b) Adams, D. J.; Topham, P. D. *Soft Matter* **2010**, *6*, 3707. (c) Dastidar, P. *Chem. Soc. Rev.* **2008**, *37*, 269. (d) Jonker, A. M.; Löwik, D. W. P. M.; van Hest, J. C. M. *Chem. Mater.* **2012**, *24*, 759.
- (6) Hartgerink, J. D.; Beniash, E.; Stupp, S. I. *Science* **2001**, *294*, 1684.
- (7) (a) Cui, H.; Webber, M. J.; Stupp, S. I. *Biopolymers* **2010**, *94*, 1. (b) Niece, K. L.; Czeisler, C.; Sahní, V.; Tysseling-Mattiace, V.; Pashuck, E. T.; Kessler, J. A.; Stupp, S. I. *Biomaterials* **2008**, *29*, 4501.
- (8) (a) Hadjichristidis, N.; Iatrou, H.; Pitsikalis, M.; Sakellariou, G. *Chem. Rev.* **2009**, *109*, 5528. (b) Deming, T. J. *Nature* **1997**, *390*, 386. (c) Habraken, G. J. M.; Peeters, M.; Dietz, C. H. J. T.; Koning, C. E.; Heise, A. *Polym. Chem.* **2010**, *1*, 514.
- (9) (a) Bertin, A.; Hermes, F.; Schlaad, H. *Adv. Polym. Sci.* **2010**, *224*, 167. (b) Cheng, J.; Deming, T. J. *Top. Curr. Chem.* **2012**, *310*, 1. (c) Habraken, G. J. M.; Heise, A.; Thornton, P. D. *Macromol. Rapid Commun.* **2012**, *33*, 272. (d) Colin, B.; Huang, J.; Ibarboure, E.; Heise, A.; Lecommandoux, S. *Chem. Commun.* **2012**, *48*, 8353. (e) Huang, J.; Bonduelle, C.; Thévenot, J.; Lecommandoux, S.; Heise, A. *J. Am. Chem. Soc.* **2012**, *134*, 119. (f) Schatz, C.; Louguet, S.; Le Meins, J.-F.; Lecommandoux, S. *Angew. Chem., Int. Ed.* **2009**, *48*, 2572.
- (10) (a) Nowak, A. P.; Breedveld, V.; Pakstis, L.; Ozbas, B.; Pine, D. J.; Pochan, D.; Deming, T. J. *Nature* **2002**, *417*, 424. (b) Breedveld, V.; Nowak, A. P.; Sato, J.; Deming, T. J.; Pine, D. J. *Macromolecules* **2004**, *37*, 3943. (c) Nowak, A. P.; Breedveld, V.; Pine, D. J.; Deming, T. J. *J. Am. Chem. Soc.* **2003**, *125*, 15666. (d) Nowak, A. P.; Sato, J.; Breedveld, V.; Deming, T. J. *Supramol. Chem.* **2006**, *18*, 423. (e) Deming, T. J. *Soft Matter* **2005**, *1*, 28. (f) Li, Z. B.; Deming, T. J. *Soft Matter* **2010**, *6*, 2546.
- (11) (a) Choi, Y. Y.; Jang, J. H.; Park, M. H.; Choi, B. G.; Chi, B.; Jeong, B. *J. Mater. Chem.* **2010**, *20*, 3416. (b) Oh, H. J.; Joo, M. K.; Sohn, Y. S.; Jeong, B. *Macromolecules* **2008**, *41*, 8204. (c) Jeong, Y.; Joo, M. K.; Bahk, K. H.; Choi, Y. Y.; Kim, H.-T.; Kim, W.-K.; Lee, H. J.; Sohn, Y. S.; Jeong, B. *J. Controlled Release* **2009**, *137*, 25. (d) Kang, E. Y.; Yeon, B.; Moon, H. J.; Jeong, B. *Macromolecules* **2012**, *45*, 2007. (e) Shinde, U. P.; Joo, M. K.; Moon, H. J.; Jeong, B. *J. Mater. Chem.* **2012**, *22*, 6072. (f) Park, M. H.; Joo, M. K.; Choi, B. G.; Jeong, B. *Acc. Chem. Res.* **2012**, *45*, 42.
- (12) Cheng, Y.; He, C.; Xiao, C.; Ding, J.; Zhuang, X.; Huang, Y.; Chen, X. *Biomacromolecules* **2012**, *13*, 2053.
- (13) (a) Lesser, G. J.; Rose, G. D. *Proteins: Struct., Funct., Genet.* **1990**, *8*, 6. (b) Glazer, A. N.; Smith, E. L. *J. Biol. Chem.* **1961**, *236*, 2948. (c) Tanford, C.; Hauenstein, J. D.; Rands, D. G. *J. Am. Chem. Soc.* **1955**, *77*, 6409. (d) Tachibana, A.; Murachi, T. *Biochemistry* **1966**, *5*, 2756.
- (14) Pace, C. N.; Horn, G.; Hebert, E. J.; Bechert, J.; Shaw, K.; Urbanikova, L.; Scholtz, J. M.; Sevcik, J. *J. Mol. Biol.* **2001**, *312*, 393.
- (15) (a) McDonald, I. K.; Thornton, J. M. *J. Mol. Biol.* **1994**, *238*, 777. (b) Boobbyer, D. N.; Goodford, P. J.; McWhinnie, P. M.; Wade, R. C. *J. Med. Chem.* **1989**, *32*, 1083. (c) Fersht, A. R.; Shi, J. P.; Knill-Jones, J.; Lowe, D. M.; Wilkinson, A. J.; Blow, D. M.; Brick, P.; Carter, P.; Waye, M. M.; Winter, G. *Nature* **1985**, *314*, 235.
- (16) Baker, E. N.; Hubbard, R. E. *Prog. Biophys. Mol. Biol.* **1984**, *44*, 97.
- (17) (a) Malencik, D. A.; Anderson, S. R. *Biochemistry* **1996**, *35*, 4375. (b) Malencik, D. A.; Anderson, S. R. *Amino Acids* **2003**, *25*, 233. (c) Elvin, C. M.; Carr, A. G.; Huson, M. G.; Maxwell, J. M.; Pearson, R. D.; Vuocolo, T.; Liyou, N. E.; Wong, D. C. C.; Merritt, D. J.; Dixon, N. E. *Nature* **2005**, *437*, 999.
- (18) Liao, S. W.; Yu, T. B.; Guan, Z. *J. Am. Chem. Soc.* **2009**, *131*, 17638.
- (19) Yu, L.; Zhang, H.; Ding, J. D. *Angew. Chem., Int. Ed.* **2006**, *45*, 2232.
- (20) Hastings, C. L.; Kelly, H. M.; Murphy, M. J.; Barry, F. P.; O'Brien, F. J.; Duffy, G. P. *J. Controlled Release* **2012**, *10*, 73.
- (21) Liu, T. C. K.; Ismail, S.; Brennan, O.; Hastings, C.; Duffy, G. P. *J. Tissue Eng. Regen. Med.* **2011**, *5*, 501.
- (22) Petka, W. A.; Harden, J. L.; McGrath, K. P.; Wirtz, D.; Tirrell, D. A. *Science* **1998**, *281*, 389.
- (23) Joo, M. K.; Park, M. H.; Choi, B. G.; Jeong, B. *J. Mater. Chem.* **2009**, *19*, 5891.
- (24) Hamley, I. W.; Cheng, G.; Castelletto, V. *Macromol. Biosci.* **2011**, *11*, 1068.
- (25) Barth, A. *Prog. Biophys. Mol. Biol.* **2000**, *74*, 141.
- (26) Rughani, R. V.; Salick, D. A.; Lamm, M. S.; Yucel, T.; Pochan, D. J.; Schneider, J. P. *Biomacromolecules* **2009**, *10*, 1295.
- (27) Kyte, J.; Doolittle, R. F. *J. Mol. Biol.* **1982**, *157*, 105.
- (28) Yu, L.; Zhang, H.; Ding, J. D. *Angew. Chem., Int. Ed.* **2006**, *45*, 2232.
- (29) Yan, C. Q.; Pochan, D. J. *Chem. Soc. Rev.* **2010**, *39*, 3528.
- (30) Tzokova, N.; Fernyhough, C. M.; Butler, M. F.; Armes, S. P.; Ryan, A. J.; Topham, P. D.; Adams, D. J. *Langmuir* **2009**, *25*, 11082.
- (31) (a) Wilcox, P. E. *Methods Enzymol.* **1970**, *19*, 64. (b) Plunkett, K. N.; Berkowski, K. L.; Moore, J. S. *Biomacromolecules* **2005**, *6*, 632.
- (32) Thornton, P. D.; McConnell, G.; Ulijn, R. V. *Chem. Commun.* **2005**, 5913.